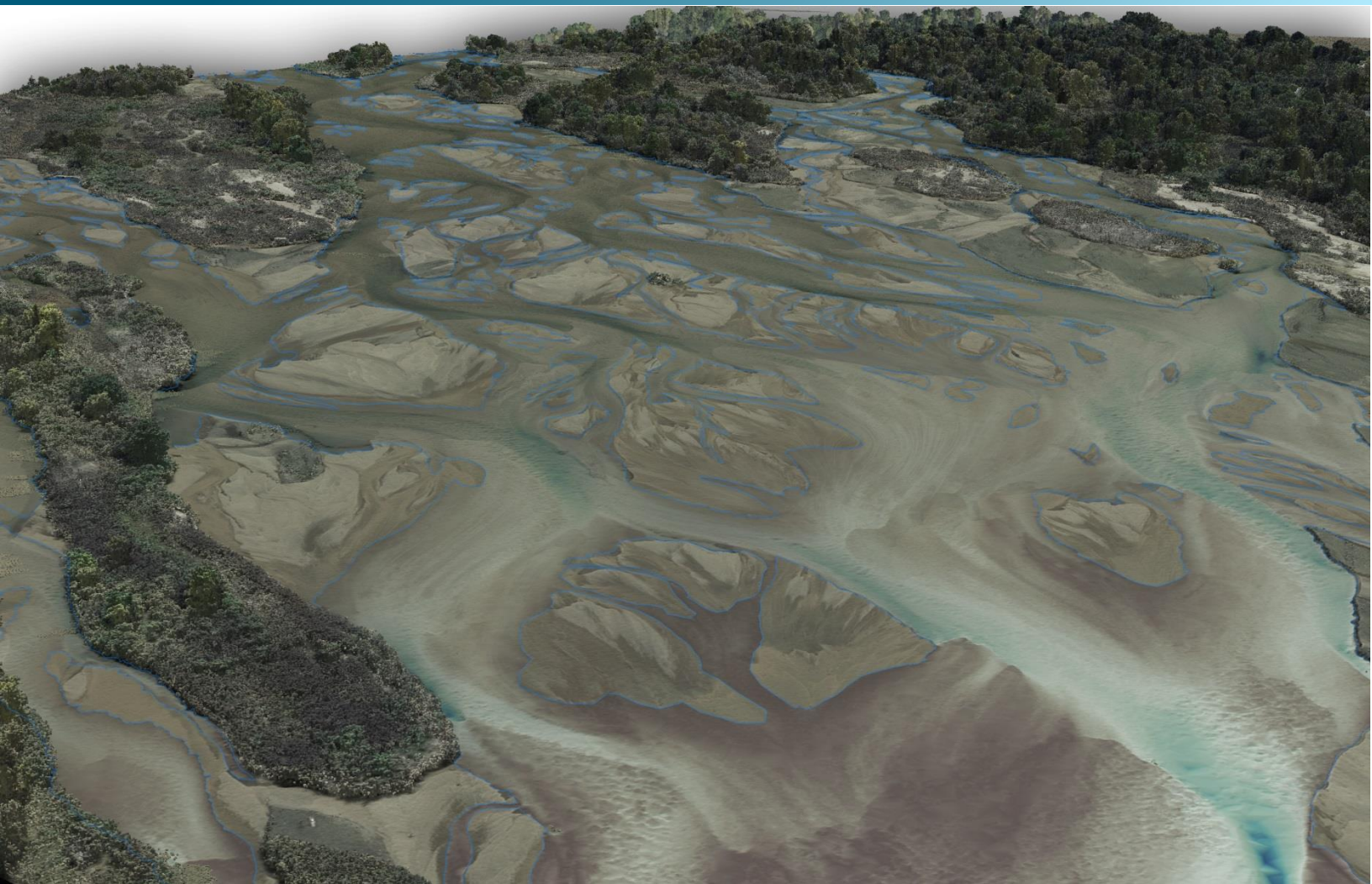


February 17, 2018



Platte River, Nebraska - Fall 2017

Topobathymetric LiDAR Technical Data Report



Justin Brei, P.E, Biosystems Engineer
Headwaters Corporation
4111 4th Avenue, Suite 6
Kearney, NE 68845
PH: 308-237-5728, ext. 4



QSI Corvallis
517 SW 2nd St., Suite 400
Corvallis, OR 97333
PH: 541-752-1204

TABLE OF CONTENTS

INTRODUCTION	1
Deliverable Products	2
ACQUISITION	4
Sensor Selection: the Riegl VQ-880-G	4
Planning.....	4
Turbidity Readings	7
Airborne LiDAR Survey	11
Ground Control.....	12
Monumentation	12
Ground Survey Points (GSPs).....	13
PROCESSING	15
Topobathymetric LiDAR Data	15
Bathymetric Refraction	17
LiDAR Derived Products.....	17
Topobathymetric DEMs	17
Intensity Images.....	18
Hydroflattening and Water’s edge breaklines.....	19
RESULTS & DISCUSSION	20
Bathymetric LiDAR.....	20
Mapped Bathymetry and Depth Penetration.....	20
LiDAR Point Density.....	21
First Return Point Density.....	21
Bathymetric and Ground Classified Point Densities	21
LiDAR Accuracy Assessments	24
LiDAR Non-Vegetated Vertical Accuracy	24
LiDAR Relative Vertical Accuracy	28
SELECTED IMAGES.....	29
GLOSSARY	30
APPENDIX A - ACCURACY CONTROLS	31

Cover Photo: A view looking over the Platte River near Burlington Northern Railroad. This image was created from the topobathymetric bare earth colored by elevation, overlaid with the above ground LiDAR returns colored using digital imagery.

INTRODUCTION

An aerial view of the Platte River within the project area, taken by QSI's airborne acquisition staff.



In 2016, Quantum Spatial (QSI) was contracted by Headwaters Corporation as part of an ongoing project (P16-009: 2016-2019 Annual LiDAR and Aerial Photography), to collect topobathymetric Light Detection and Ranging (LiDAR) data in the fall of 2017 for the Platte River site in Nebraska. The collected digital imagery was provided to Headwater's Corporation on November 28th, 2017; this report accompanies the delivered topobathymetric LiDAR data. Traditional near-infrared (NIR) LiDAR was fully integrated with green wavelength return data (bathymetric LiDAR) in order to provide seamless and complete project mapping. Data were collected to aid Headwaters Corporation in assessing the geophysical properties of the study area to support the Platte River Recovery Implementation Program, which aims to enhance, restore, and protect habitat for the Whooping Crane, Least Tern, Piping Plover, and Pallid Sturgeon species within the project area.

This report accompanies the delivered topobathymetric LiDAR data, and documents contract specifications, data acquisition procedures, processing methods, and analysis of the final dataset including LiDAR accuracy and density. Acquisition dates and acreage are shown in Table 1, a complete list of contracted deliverables provided to Headwaters Corporation is shown in Table 2, and the project extent is shown in Figure 1.

Table 1: Acquisition dates, acreage, and data types collected on the Platte River site

Project Site	Contracted Acres	Buffered Acres	Acquisition Dates	Data Type
Platte River, Nebraska	81,900	89,931	10/15/17 – 10/18/17	LiDAR

Deliverable Products

Table 2: Products delivered to Headwaters Corporation for the Platte River site

Platte River Fall 2017 LiDAR Products	
Projection: Nebraska State Plane	
Horizontal Datum: NAD83 (2011)	
Vertical Datum: NAVD88 (GEOID03)	
Units: US Survey Feet	
Topobathymetric LiDAR	
Points	LAS v 1.4 <ul style="list-style-type: none"> All Classified Returns
Rasters	3.0 Foot ESRI Grids and ERDAS Imagine Files <ul style="list-style-type: none"> Topobathymetric Bare Earth Digital Elevation Model (DEM) Bare Earth and Water Surface Digital Elevation Model (DEM), with Hydroflattened ponds Highest Hit Digital Surface Model (DSM) Topobathymetric Depth Model 1.5 Foot GeoTiffs <ul style="list-style-type: none"> Green Sensor Intensity Image NIR Sensor Intensity Image
Vectors	Shapefiles (*.shp) <ul style="list-style-type: none"> Area of Interest LiDAR Tile Index DEM Tile Index Bathymetric Coverage Polygon Hydroflattened Pond Breaklines with Z values Water's Edge Breaklines without Z values (used in refraction) Ground Survey Points and Monument Locations

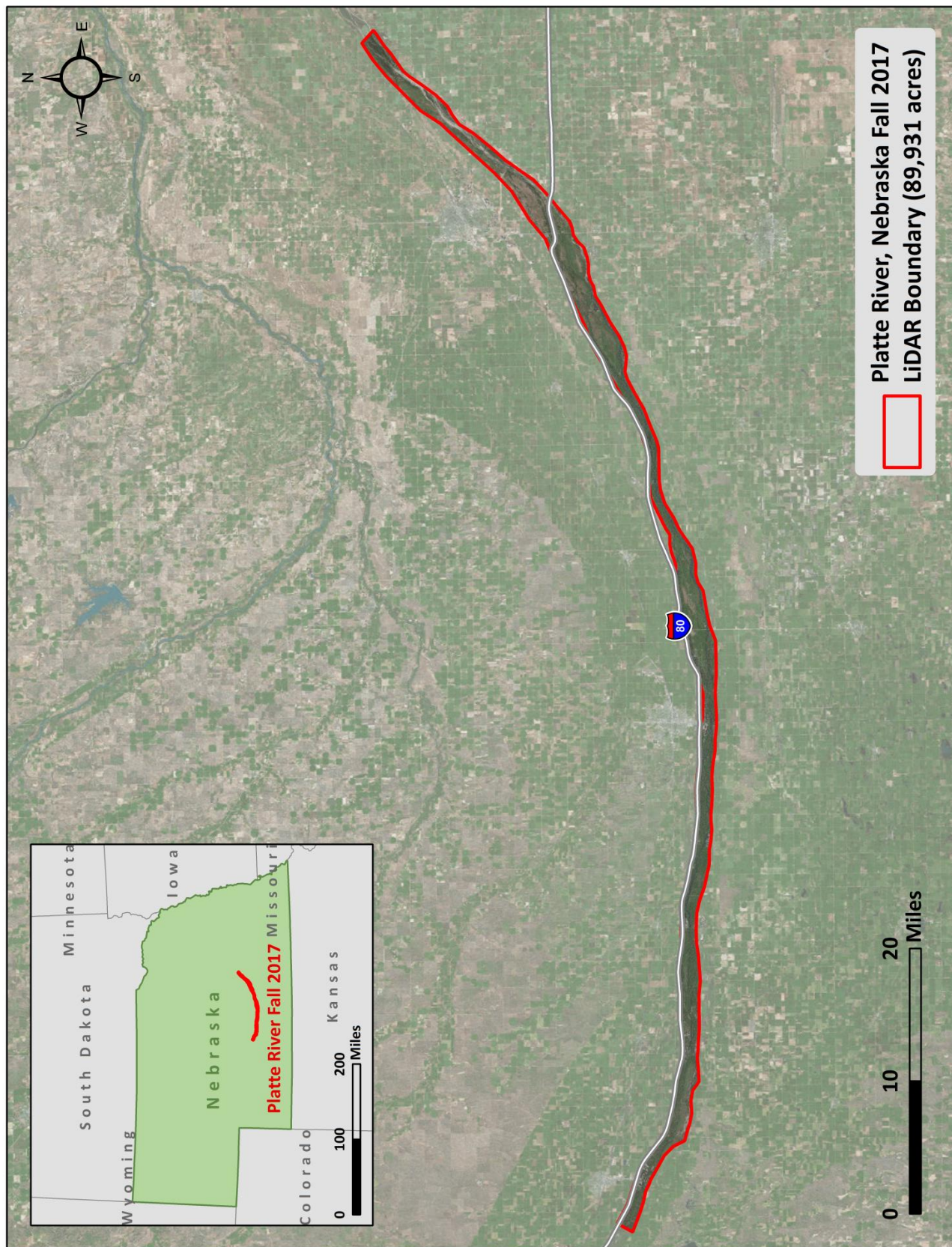


Figure 1: Location map of the Platte River site in Nebraska

Water clarity conditions in a portion of the Platte River LiDAR study area.



Sensor Selection: the Riegl VQ-880-G

The Riegl VQ-880-G was selected as the hydrographic airborne laser scanner for the Platte River project based on fulfillment of several considerations deemed necessary for effective mapping of the project site. A higher repetition pulse rate (up to 550 kHz), higher scanning speed, small laser footprint, and wide field of view allow for seamless collection of high resolution data of both topographic and bathymetric surfaces. A short laser pulse length allows for discrimination of underwater surface expression in shallow water, critical to shallow and dynamic environments such as the Platte River. Sensor specifications and settings for the Platte River acquisition are displayed in Table 3.

Planning

In preparation for data collection, QSI reviewed the project area and developed a specialized flight plan to ensure complete coverage of the Platte River LiDAR study area at the target point density of ≥ 6.0 points/m². Acquisition parameters including orientation relative to terrain, flight altitude, pulse rate, scan angle, and ground speed were adapted to optimize flight paths and flight times while meeting all contract specifications.

Factors such as satellite constellation availability and weather windows must be considered during the planning stage. Any weather hazards or conditions affecting the flight were continuously monitored due to their potential impact on the daily success of airborne and ground operations. In addition, logistical considerations including private property access, potential air space restrictions, channel flow rates (Figure 2 and Figure 3), and water clarity were reviewed.

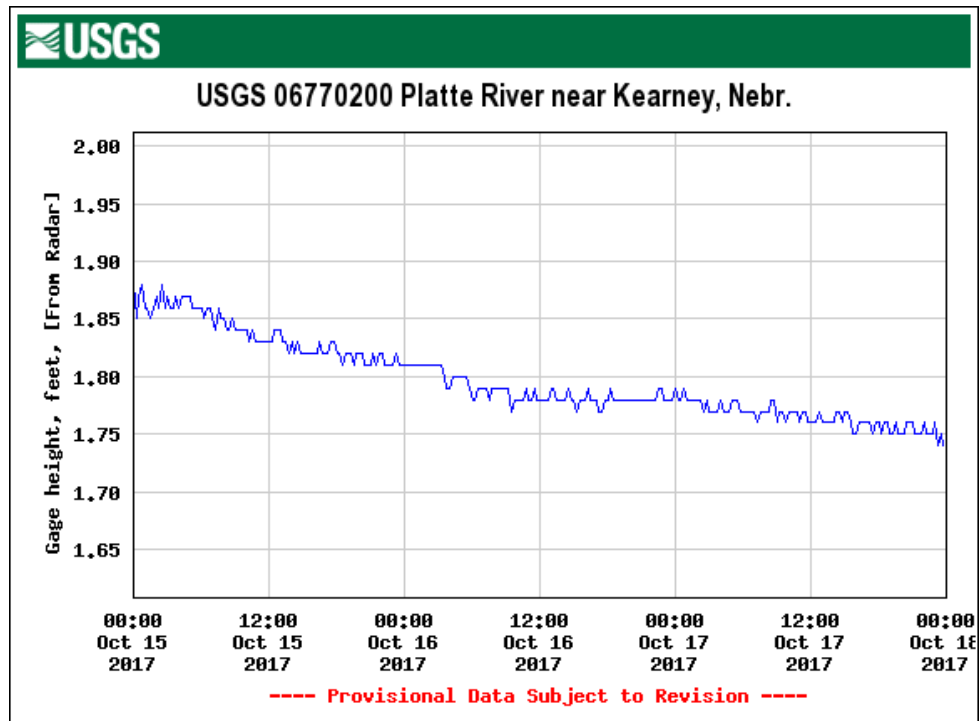


Figure 2: USGS Station 06770200 flow rates along the Platte River at the time of LiDAR acquisition

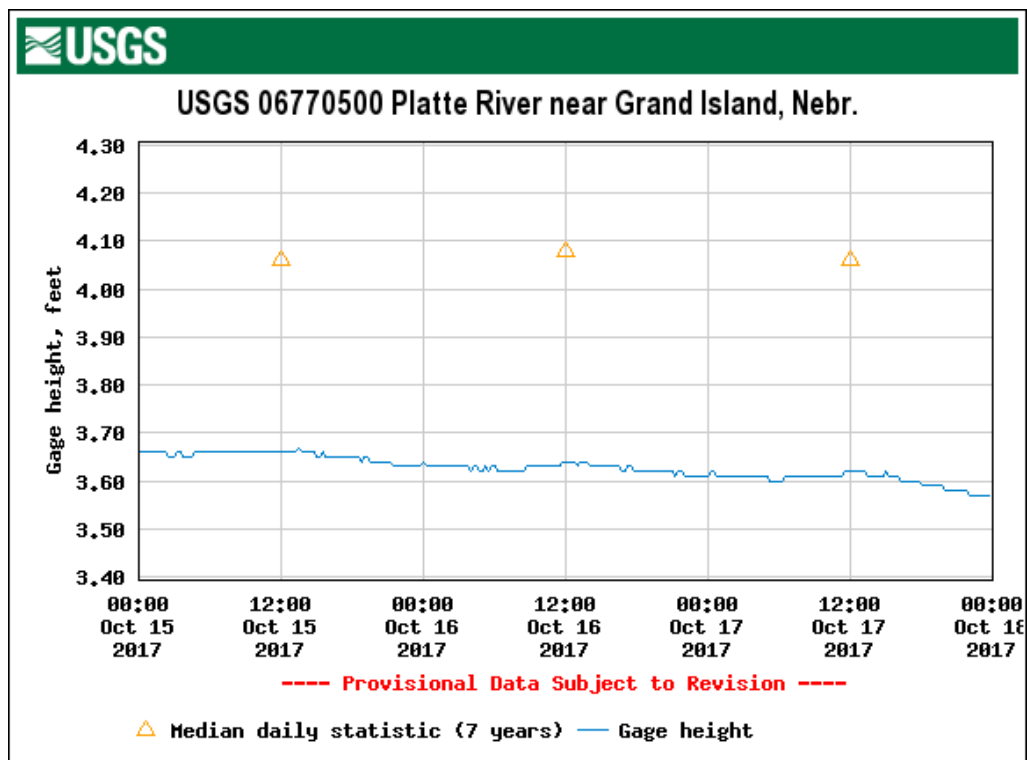








Figure 3: USGS Station 06770500 gauge height along the Platte River at the time of LiDAR acquisition



Figure 4: These photos taken by QSI acquisition staff display water clarity conditions at two locations within the Platte River site.

Turbidity Readings

Turbidity Location	Date	Depth of Turbidity Reading	Average Turbidity Reading (NTU)	Photo
1	10/16/2017	15 cm	6.42	
1	10/16/2017	25 cm	7.16	
1	10/16/2017	45 cm	7.70	

Turbidity Location	Date	Depth of Turbidity Reading	Average Turbidity Reading (NTU)	Photo
2	10/16/2017	10 cm	4.15	
2	10/16/2017	20 cm	3.37	
2	10/16/2017	45 cm	3.67	

Turbidity Location	Date	Depth of Turbidity Reading	Average Turbidity Reading (NTU)	Photo
3	10/18/2017	15 cm	7.08	
3	10/18/2017	25 cm	6.98	
3	10/18/2017	45 cm	6.03	

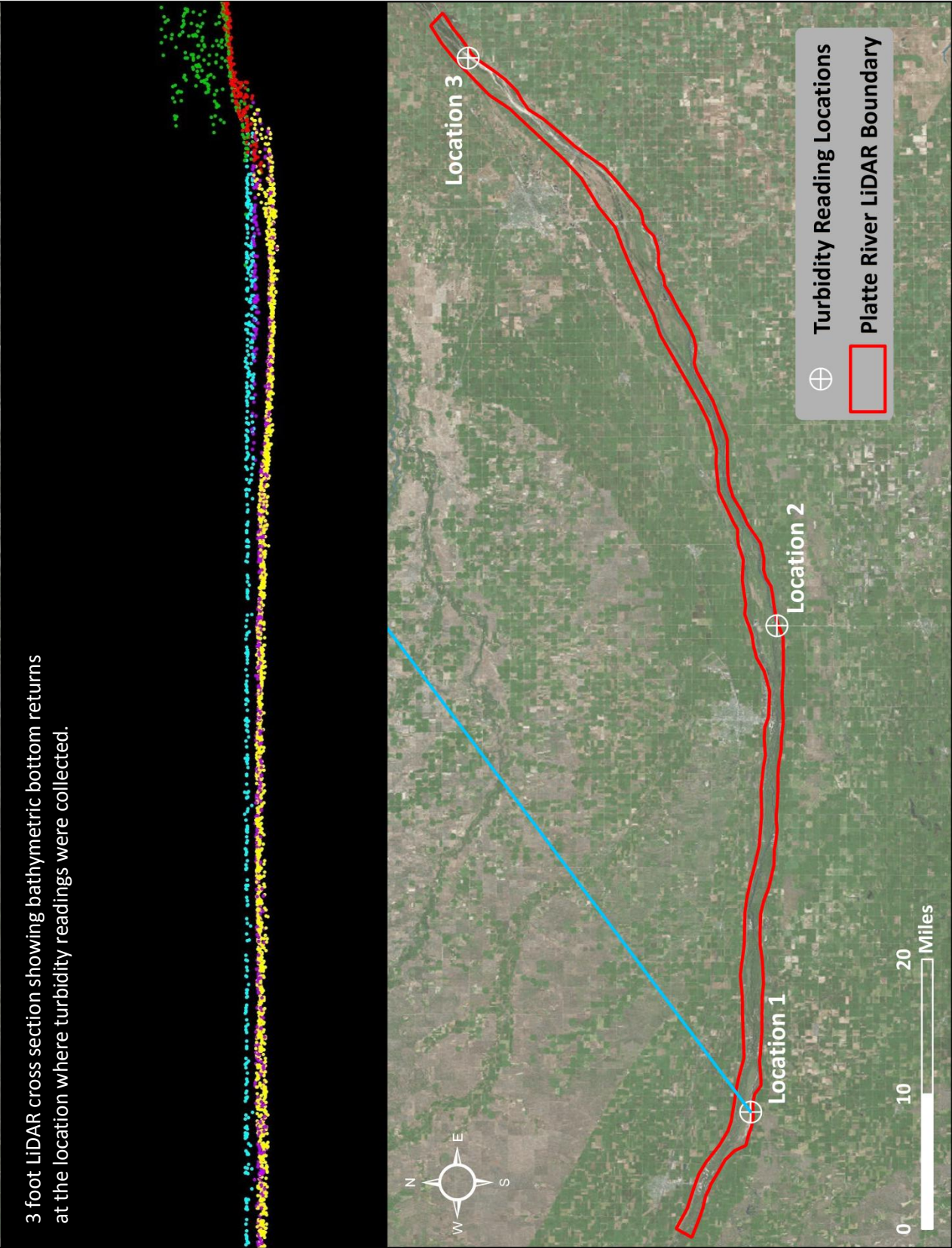


Figure 5: Turbidity reading location map

Airborne LiDAR Survey

The LiDAR survey was accomplished using a Riegl VQ-880-G topobathymetric sensor mounted in a Cessna Caravan. The Riegl VQ-880-G uses a green wavelength ($\lambda=532$ nm) laser that is capable of collecting high resolution vegetation and topography data, as well as penetrating the water surface with minimal spectral absorption by water. The Riegl VQ-880-G contains an integrated NIR laser ($\lambda=1064$ nm) that adds additional topography data and aids in water surface modeling. The recorded waveform enables range measurements for all discernible targets for a given pulse. The typical number of returns digitized from a single pulse range from 1 to 7 for the Platte River project area. It is not uncommon for some types of surfaces (e.g., dense vegetation or water) to return fewer pulses to the LiDAR sensor than the laser originally emitted. The discrepancy between first return and overall delivered density will vary depending on terrain, land cover, and the prevalence of water bodies. All discernible laser returns were processed for the output dataset. Table 3 summarizes the settings used to yield an average pulse density of ≥ 6 pulses/m² over the Platte River project area.

Table 3: LiDAR specifications and survey settings

LiDAR Survey Settings & Specifications		
Acquisition Dates	10/15/2017 – 10/18/17	10/15/2017 – 10/18/17
Aircraft Used	Cessna Caravan	Cessna Caravan
Sensor	Riegl	Riegl
Laser	VQ-880-G	VQ-880-G-IR
Maximum Returns	Unlimited	Unlimited
Resolution/Density	Average 6 pulses/m ²	Average 6 pulses/m2
Nominal Pulse Spacing	0.41 m	0.41 m
Survey Altitude (AGL)	450 m	450 m
Survey speed	110 knots	110 knots
Field of View	40°	40°
Mirror Scan Rate	80 lines per second	Uniform point spacing
Target Pulse Rate	245 kHz	245 kHz
Pulse Length	1.5 ns	3 ns
Laser Pulse Footprint Diameter	45 cm	9 cm
Central Wavelength	532 nm	1064 nm
Pulse Mode	MTA (multiple times around)	MTA (multiple times around)
Beam Divergence	0.7 mrad	0.2 mrad
Swath Width	328 m	328 m
Swath Overlap	55%	55%
Intensity	16-bit	16-bit
Accuracy	RMSE _z ≤ 25 cm	RMSE _z ≤ 25 cm

All areas were surveyed with an opposing flightline side-lap of $\geq 50\%$ ($\geq 100\%$ overlap) in order to reduce laser shadowing and increase surface laser painting. To accurately solve for laser point position (geographic coordinates x, y, and z), the positional coordinates of the airborne sensor and the attitude of the aircraft were recorded continuously throughout the LiDAR data collection mission. Position of the

aircraft was measured twice per second (2 Hz) by an onboard differential GPS unit, and aircraft attitude was measured 200 times per second (200 Hz) as pitch, roll, and yaw (heading) from an onboard inertial measurement unit (IMU). To allow for post-processing correction and calibration, aircraft and sensor position and attitude data are indexed by GPS time.

Ground Control

Ground control surveys were conducted to support the airborne acquisition. Ground control data were used to geospatially correct and perform quality assurance checks on final LiDAR data products. In addition, a permanent base station was utilized to geospatially correct the aircraft positional coordinate data and to support ground survey point (GSP) collection.



Existing QSI Monument

Monumentation

The spatial configuration of base stations provided redundant control within 13 nautical miles of the mission areas for LiDAR flights (Table 4, Figure 6). Base stations were also used for collection of ground survey points using real time kinematic (RTK) survey techniques.

Two permanent base stations from the Trimble VRS Now Real-Time Network (RTN) were utilized for the Platte River airborne acquisition and RTK survey. In addition, QSI utilized eight existing monuments, of which seven were established by QSI in 2016. Monument locations were selected with consideration for satellite visibility, field crew safety, and optimal location for GSP coverage.

Table 4: Monuments established for the Platte River acquisition. Coordinates are on the NAD83 (2011) datum, epoch 2010.00.

Monument ID	Origin	Latitude	Longitude	Ellipsoid (meters)
LH1439	NGS	40° 42' 50.87194"	-99° 21' 00.62321"	662.992
NEDO	VRS-Now Base	40° 46' 39.11703"	-98° 22' 36.49354"	576.962
NELN	VRS-Now Base	40° 46' 05.66516"	-99° 42' 43.38894"	708.806
PLATTE_RIVER_02	QSI 2016	40° 41' 44.14257"	-99° 32' 26.55836"	679.971
PLATTE_RIVER_03	QSI 2016	40° 39' 05.51638"	-99° 05' 07.57789"	629.072
PLATTE_RIVER_04	QSI 2016	40° 40' 42.05134"	-98° 57' 05.26828"	615.159
PLATTE_RIVER_06	QSI 2016	40° 44' 36.62855"	-98° 35' 09.49188"	572.813
PLATTE_RIVER_07	QSI 2016	40° 47' 23.41263"	-98° 29' 34.40987"	562.656
PLATTE_RIVER_08	QSI 2016	40° 53' 03.62608"	-98° 17' 17.04589"	535.189
PLATTE_RIVER_09	QSI 2016	40° 55' 50.47020"	-98° 10' 10.32711"	543.957

To correct the continuously recorded onboard measurements of the aircraft position, QSI concurrently conducted multiple static Global Navigation Satellite System (GNSS) ground surveys (1 Hz recording frequency) over each monument. During post-processing, the static GPS data were triangulated with

nearby CORS using the Online Positioning User Service (OPUS¹) for precise positioning. Multiple independent sessions over the same monument were processed to confirm antenna height measurements and to refine position accuracy.

Monuments were established according to the national standard for geodetic control networks, as specified in the Federal Geographic Data Committee (FGDC) Geospatial Positioning Accuracy Standards for geodetic networks.² This standard provides guidelines for classification of monument quality at the 95% confidence interval as a basis for comparing the quality of one control network to another. The monument rating for this project is shown in Table 5.

Table 5: Federal Geographic Data Committee monument rating for network accuracy

Direction	Rating
1.96 * St Dev _{NE} :	0.020 m
1.96 * St Dev _z :	0.050 m

For the Platte River LiDAR project, the monument coordinates contributed no more than 5.4 cm of positional error to the geolocation of the final ground survey points and LiDAR, with 95% confidence.

Ground Survey Points (GSPs)

Ground survey points were collected using real time kinematic survey (RTK) techniques. A Trimble VRS-Now base station or QSI-owned Trimble R7 base unit was positioned at a nearby monument to broadcast a kinematic correction to a roving Trimble R10 receiver. All GSP measurements were made during periods with a Position Dilution of Precision (PDOP) of ≤ 3.0 with at least six satellites in view of the stationary and roving receivers. When collecting RTK and PPK data, the rover records data while stationary for five seconds, then calculates the pseudorange position using at least three one-second epochs. Relative errors for any GSP position must be less than 1.5 cm horizontal and 2.0 cm vertical in order to be accepted. See Table 6 for Trimble unit specifications.

GSPs were collected in areas where good satellite visibility was achieved on paved roads and other hard surfaces such as gravel or packed dirt roads. GSP measurements were not taken on highly reflective surfaces such as center line stripes or lane markings on roads due to the increased noise seen in the laser returns over these surfaces. GSPs were collected within as many flightlines as possible; however the distribution of GSPs depended on ground access constraints and monument locations and may not be equitably distributed throughout the study area (Figure 6).

Table 6: Trimble equipment identification

Receiver Model	Antenna	OPUS Antenna ID	Use
Trimble Net R9	Zephyr GNSS Geodetic Model II	TRM55971.00	Trimble VRS-Now
Trimble R7 GNSS	Zephyr GNSS Geodetic Model 2 RoHS	TRM57971.00	Static
Trimble R10	Integrated Antenna R10	TRMR10	Static, Rover

¹ OPUS is a free service provided by the National Geodetic Survey to process corrected monument positions. <http://www.ngs.noaa.gov/OPUS/>.

² Federal Geographic Data Committee, Geospatial Positioning Accuracy Standards (FGDC-STD-007.2-1998). Part 2: Standards for Geodetic Networks, Table 2.1, page 2-3. <http://www.fgdc.gov/standards/projects/FGDC-standards-projects/accuracy/part2/chapter2>

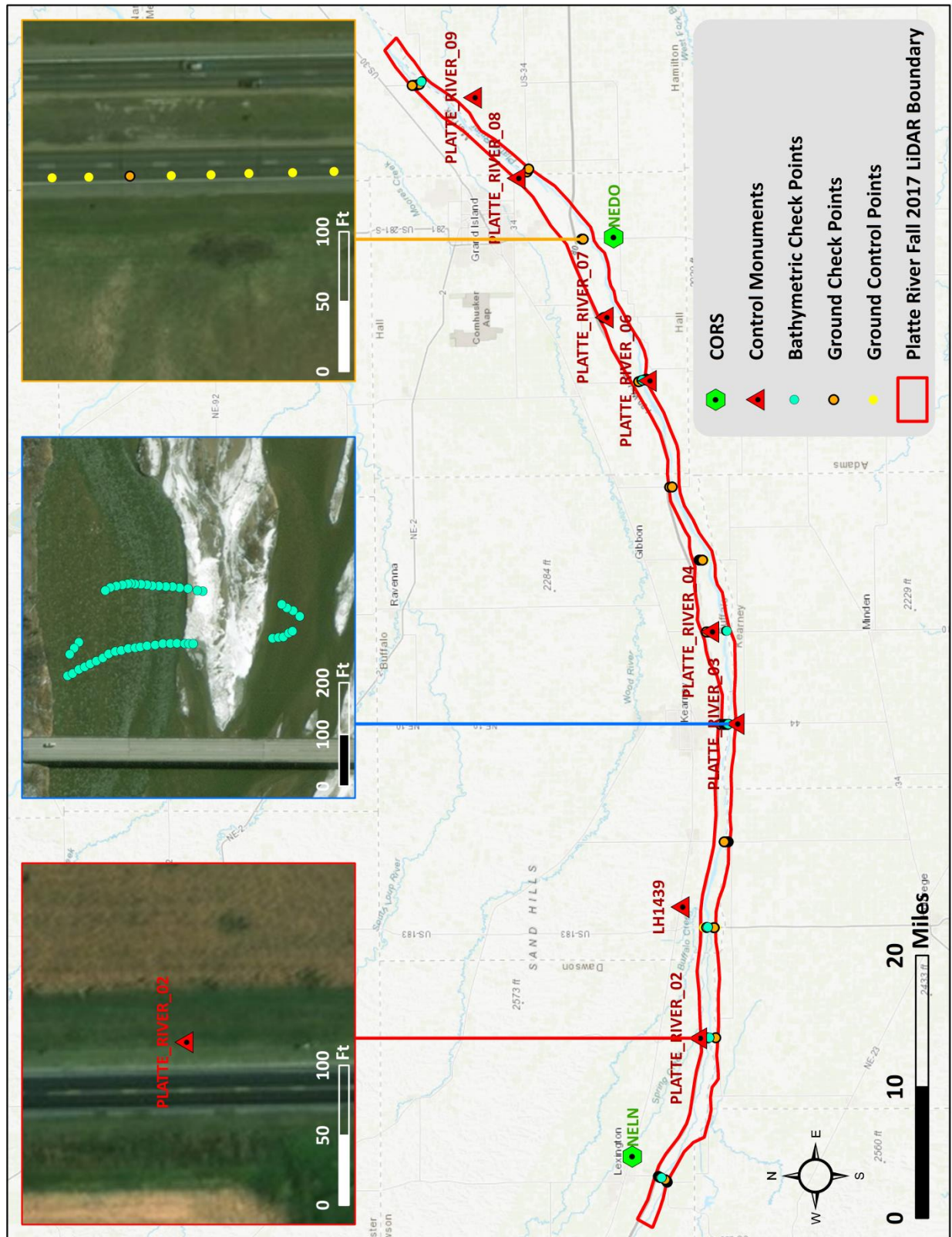
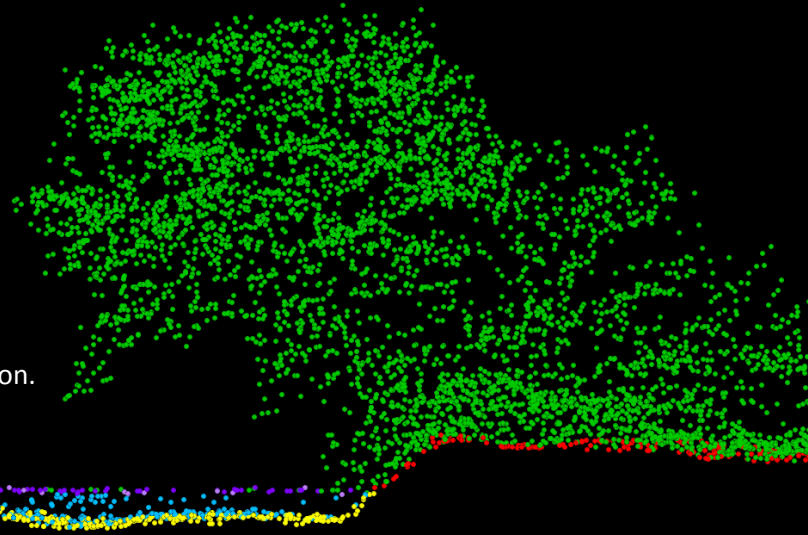


Figure 6: Ground survey location map

Default
 Ground
 NIR Water Surface
 Water Column
 Green Water Surface
 Bathymetric Bottom

This 6 foot LiDAR cross-section shows a view of the Platte River point cloud colored by point classification.



Topobathymetric LiDAR Data

Upon completion of data acquisition, QSI processing staff initiated a suite of automated and manual techniques to process the data into the requested deliverables. Processing tasks included GPS control computations, smoothed best estimate trajectory (SBET) calculations, kinematic corrections, calculation of laser point position, sensor and data calibration for optimal relative and absolute accuracy, and LiDAR point classification (Table 7).

Riegl's RiProcess software was used to facilitate bathymetric return processing. Once bathymetric points were differentiated, they were spatially corrected for refraction through the water column based on the angle of incidence of the laser. QSI refracted water column points using QSI's proprietary LAS processing software, LAS Monkey. The resulting point cloud data were classified using both manual and automated techniques. Processing methodologies were tailored for the landscape. Brief descriptions of these tasks are shown in Table 8.

Table 7: ASPRS LAS classification standards applied to the Platte River dataset

Classification Number	Classification Name	Classification Description
1	Default/Unclassified	Laser returns that are not included in the ground class, composed of vegetation and anthropogenic features.
2	Ground	Laser returns that are determined to be ground using automated and manual cleaning algorithms.
7W	Noise	Laser returns that are often associated with birds, scattering from reflective surfaces, or artificial points below the ground surface.

Classification Number	Classification Name	Classification Description
9	Water	NIR laser returns that are determined to be water using automated and manual cleaning algorithms.
12WO	Overlap	Flightline edge overlap clipped to maintain contracted scan angles.
25	Water Column	Refracted Riegl sensor returns that are determined to be water using automated and manual cleaning algorithms.
26	Bathymetric Bottom	Refracted Riegl sensor returns that fall within the water's edge breakline which characterize the submerged topography.
27	Water Surface	Green laser returns that are determined to be water surface points using automated and manual cleaning algorithms.

Table 8: LiDAR processing workflow

LiDAR Processing Step	Software Used
Resolve kinematic corrections for aircraft position data using kinematic aircraft GPS and static ground GPS data. Develop a smoothed best estimate of trajectory (SBET) file that blends post-processed aircraft position with sensor head position and attitude recorded throughout the survey.	POSPac MMS v7.1 SP3
Calculate laser point position by associating SBET position to each laser point return time, scan angle, intensity, etc. Create raw laser point cloud data for the entire survey in *.las (ASPRS v. 1.2) format. Convert data to orthometric elevations by applying a geoid correction.	RiProcess v1.8.2 TerraMatch v.17
Import raw laser points into manageable blocks (less than 500 MB) to perform manual relative accuracy calibration and filter erroneous points. Classify ground points for individual flightlines.	TerraScan v.17
Using ground classified points per each flightline, test the relative accuracy. Perform automated line-to-line calibrations for system attitude parameters (pitch, roll, heading), mirror flex (scale) and GPS/IMU drift. Calculate calibrations on ground classified points from paired flightlines and apply results to all points in a flightline. Use every flightline for relative accuracy calibration.	TerraMatch v.17 RiProcess v1.8.2
Apply refraction correction to all subsurface returns.	LAS Monkey 2.2.7SP1 (QSI proprietary software)
Classify resulting data to ground and other client designated ASPRS classifications (Table 7). Assess statistical absolute accuracy via direct comparisons of ground classified points to ground control survey data.	TerraScan v.17 TerraModeler v.17
Generate bare earth models as triangulated surfaces. Generate highest hit models as a surface expression of all classified points. Export all surface models as ESRI GRIDs in EDRAS Imagine (.img) format at a 3.0 foot pixel resolution.	TerraScan v.17 TerraModeler v.17 ArcMap v. 10.2.2
Export intensity images as GeoTIFFs at a 1.5 foot pixel resolution.	ArcMap v. 10.2.2 Las Product Creator 1.5 (QSI proprietary software)

Bathymetric Refraction

The water surface model used for refraction is generated using NIR points within the breaklines defining the water's edge. Points are filtered and edited to obtain the most accurate representation of the water surface and are used to create a water surface model TIN. A tin model is preferable to a raster based water surface model to obtain the most accurate angle of incidence during refraction. The refraction processing is done using Las Monkey; QSI's proprietary LiDAR processing tool. After refraction, the points are compared against bathymetric control points to assess accuracy.

LiDAR Derived Products

Because hydrographic laser scanners penetrate the water surface to map submerged topography, this affects how the data should be processed and presented in derived products from the LiDAR point cloud. The following discusses certain derived products that vary from the traditional (NIR) specification and delivery format.

Topobathymetric DEMs

Bathymetric bottom returns can be limited by depth, water clarity, and bottom surface reflectivity. Water clarity and turbidity affects the depth penetration capability of the green wavelength laser with returning laser energy diminishing by scattering throughout the water column. Additionally, the bottom surface must be reflective enough to return remaining laser energy back to the sensor at a detectable level. It is not unexpected to have no bathymetric bottom returns in turbid or non-reflective areas. As a result, creating digital elevation models (DEMs) presents a challenge with respect to interpolation of areas with no returns. In traditional DEM creation areas lacking ground returns are interpolated from neighboring ground returns (or breaklines in the case of hydro-flattening), with the assumption that the interpolation is close to reality. In bathymetric modeling, these assumptions are prone to error because a lack of bathymetric returns can indicate a change in elevation that the laser can no longer map due to increased depths. The resulting void areas may suggest greater depths, rather than similar elevations from neighboring bathymetric bottom returns. Therefore, QSI created a water polygon with bathymetric coverage to delineate areas with successfully mapped bathymetry. This shapefile was provided along with the topobathymetric DEM, and may be used to control the extent of the topobathymetric model to avoid false triangulation (interpolation from TIN'ing) across areas in the water with no bathymetric returns.

Intensity Images

The difference in emitted wavelengths of the NIR (1064 nm) and Green (532 nm) lasers results in variation of the intensity information returned to the sensor for each laser. Additionally, the near-infrared wavelength is subject to spectral absorption by water, which can result in no returns over water surfaces. Due to these factors, QSI created one set of intensity images from NIR laser first returns, and one set of intensity images from green laser first returns in order to provide the most useful intensity information. The difference in intensity images is displayed in (Figure 7).

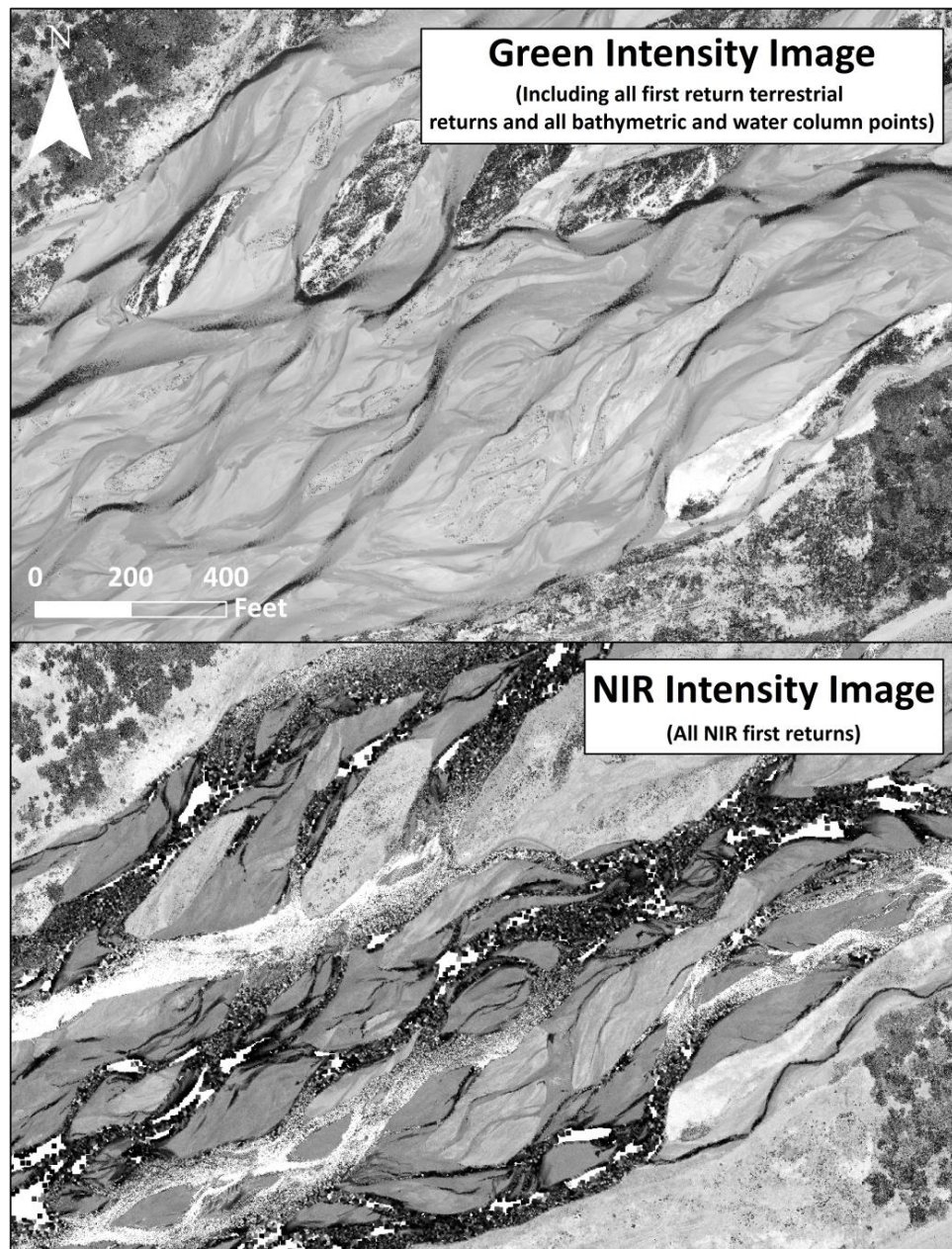


Figure 7: A comparison of Intensity Images from Green and NIR returns in the Platte River area

Hydroflattening and Water's edge breaklines

The Platte River, and any lakes and ponds outside of the area's main river channel were flattened to a consistent water level. The hydroflattening process eliminates artifacts in the digital terrain model caused by both increased variability in ranges or dropouts in laser returns due to the low reflectivity of water.

Hydroflattening of closed water bodies was performed through a combination of automated and manual detection and adjustment techniques designed to identify water boundaries and water levels. Boundary polygons were developed using an algorithm which weights LiDAR-derived slopes, intensities, and return densities to detect the water's edge. The water edges were then manually reviewed and edited as necessary.

Once polygons were developed, the initial ground classified points falling within water polygons were reclassified as water points to omit them from the final ground model. Elevations were then obtained from the filtered LiDAR returns to create the final breaklines. Lakes were assigned a consistent elevation for the entire polygon. Water boundary breaklines were then incorporated into the hydroflattened DEM by enforcing triangle edges (adjacent to the breakline) to the elevation values of the breakline. This implementation corrected interpolation along the hard edge. Water surfaces were obtained from a TIN of the 3-D water edge breaklines resulting in the final hydroflattened model (Figure 8).

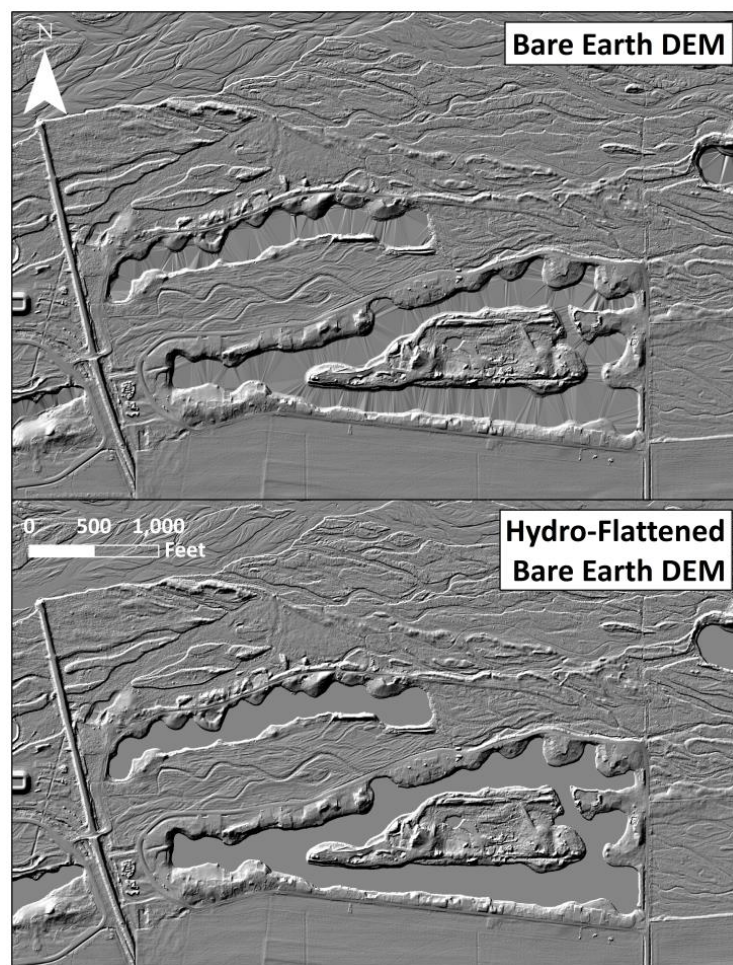
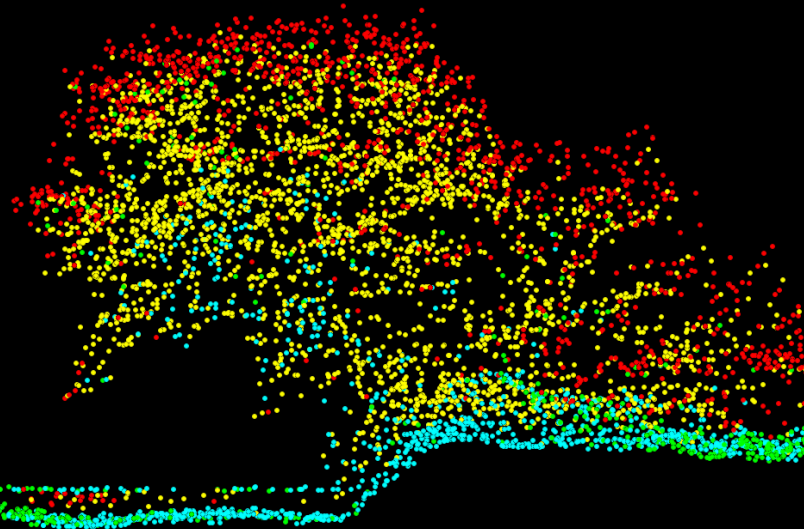


Figure 8: Example of hydro-flattening in the Platte River LiDAR dataset

Only Echo 
First of Many 
Intermediate 
Last of Many 

This 6 foot LiDAR cross-section shows a view of the Platte River point cloud colored by laser echo.



Bathymetric LiDAR

An underlying principle for collecting hydrographic LiDAR data is to survey near-shore areas that can be difficult to collect with other methods, such as multi-beam sonar, particularly over large areas. In order to determine the capability and effectiveness of the bathymetric LiDAR, several parameters were considered; depth penetrations below the water surface, bathymetric return density, and spatial accuracy.

Mapped Bathymetry and Depth Penetration

To assist in evaluating performance results of the sensor, a polygon layer was created to delineate areas where bathymetry was successfully mapped. Insufficiently mapped areas were identified by triangulating bathymetric bottom points with an edge length maximum of 15.2 feet. This ensured all areas of no returns ($> 100 \text{ ft}^2$), were identified as data voids. For the Platte River project a maximum depth of 24.36 feet was achieved. QSI has provided a depth raster, which was created by subtracting the topobathymetric bare earth model from the water surface model and clipping the resulting raster to the covered areas within the bathymetric coverage shape. Additionally, QSI successfully mapped over 99% of the main river channel within the Platte River study area.

LiDAR Point Density

First Return Point Density

The acquisition parameters were designed to acquire an average first-return density of 6 points/m². First return density describes the density of pulses emitted from the laser that return at least one echo to the system. Multiple returns from a single pulse were not considered in first return density analysis. Some types of surfaces (e.g., breaks in terrain, water and steep slopes) may have returned fewer pulses than originally emitted by the laser.

First returns typically reflect off the highest feature on the landscape within the footprint of the pulse. In forested or urban areas the highest feature could be a tree, building or power line, while in areas of unobstructed ground, the first return will be the only echo and represents the bare earth surface.

The average first-return density of the Platte River LiDAR project was 2.66 points/ft² (28.68 points/m²) (Table 9). The statistical and spatial distributions of all first return densities per 100 m x 100 m cell are portrayed in Figure 9 and Figure 11.

Bathymetric and Ground Classified Point Densities

The density of ground classified LiDAR returns and bathymetric bottom returns were also analyzed for this project. Terrain character, land cover, and ground surface reflectivity all influenced the density of ground surface returns. In vegetated areas, fewer pulses may have penetrated the canopy, resulting in lower ground density. Similarly, the density of bathymetric bottom returns was influenced by turbidity, depth, and bottom surface reflectivity. In turbid areas, fewer pulses may have penetrated the water surface, resulting in lower bathymetric density.

The ground and bathymetric bottom classified density of LiDAR data for the Platte River project was 0.94 points/ft² (10.10 points/m²) (Table 9). The statistical and spatial distributions ground classified and bathymetric bottom return densities per 100 m x 100 m cell are portrayed in Figure 10 and Figure 11.

Additionally, for the Platte River project, density values of only bathymetric bottom returns were calculated for areas containing at least 1 bathymetric bottom return. These values are included in the bathymetric coverage shapefile. Areas lacking bathymetric returns were not considered in calculating an average density value. Within the successfully mapped area, a bathymetric bottom return density of 1.16 points/ft² (12.53 points/m²) was achieved.

Table 9: Average LiDAR point densities

Density Type	Point Density
Green and NIR Laser First Returns	2.66 points/ft ² 28.68 points/m ²
Ground and Bathymetric Bottom Classified Returns	0.94 points/ft ² 10.10 points/m ²
Bathymetric Bottom Classified Returns	1.16 points/ft ² 12.53 points/m ²

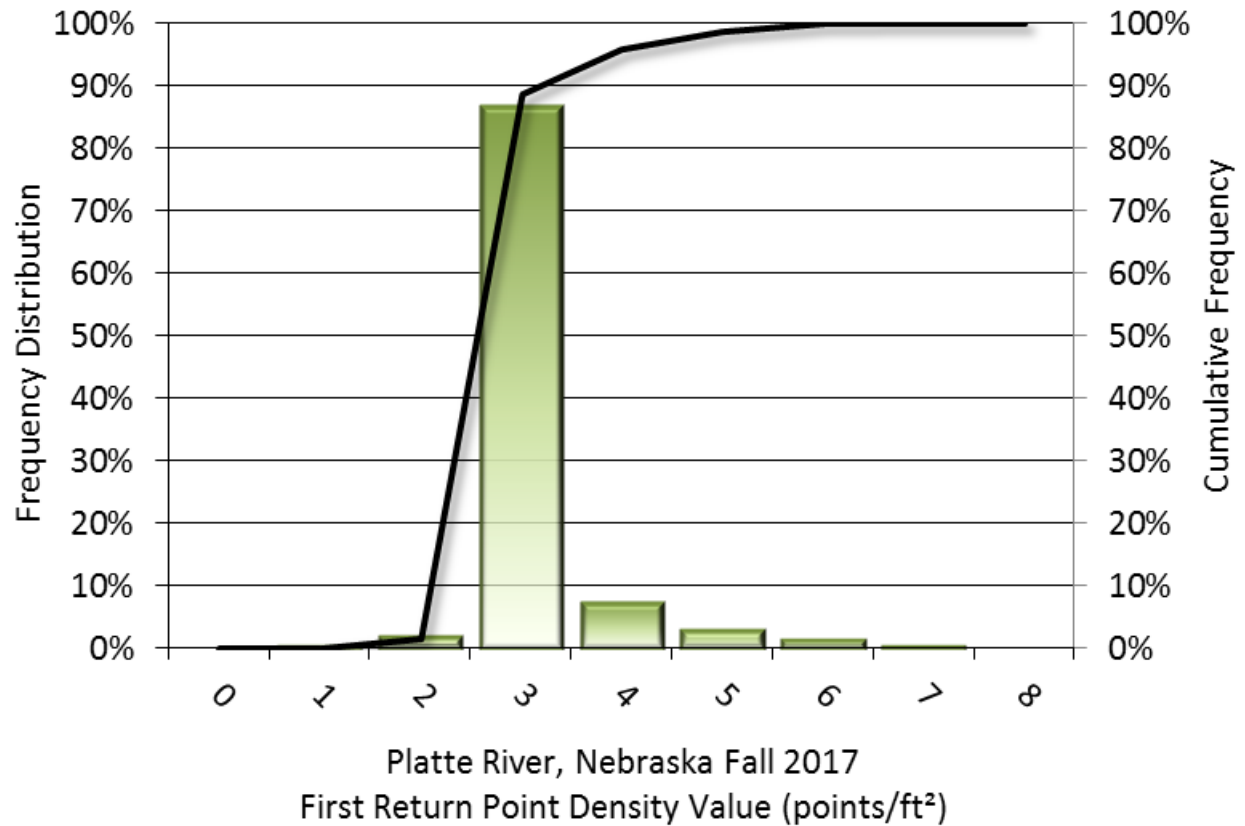


Figure 9: Frequency distribution of first return densities per 100 x 100 m cell

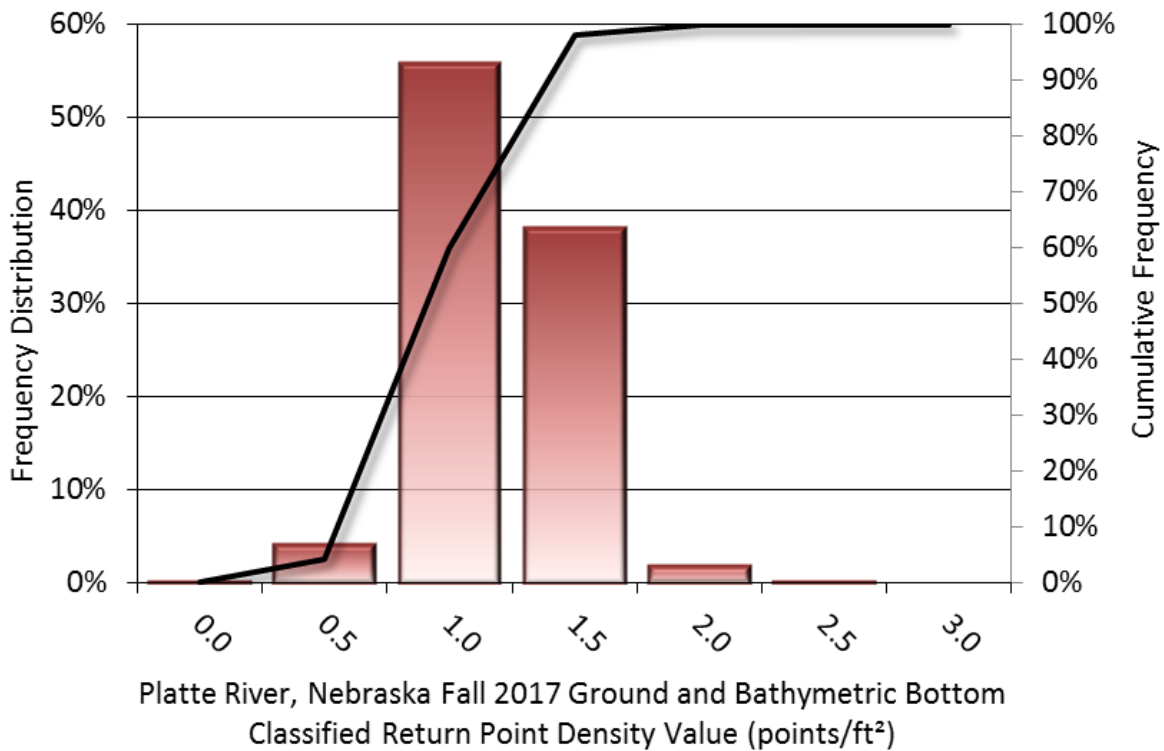


Figure 10: Frequency distribution of ground and bathymetric bottom classified return densities per 100 x 100 m cell

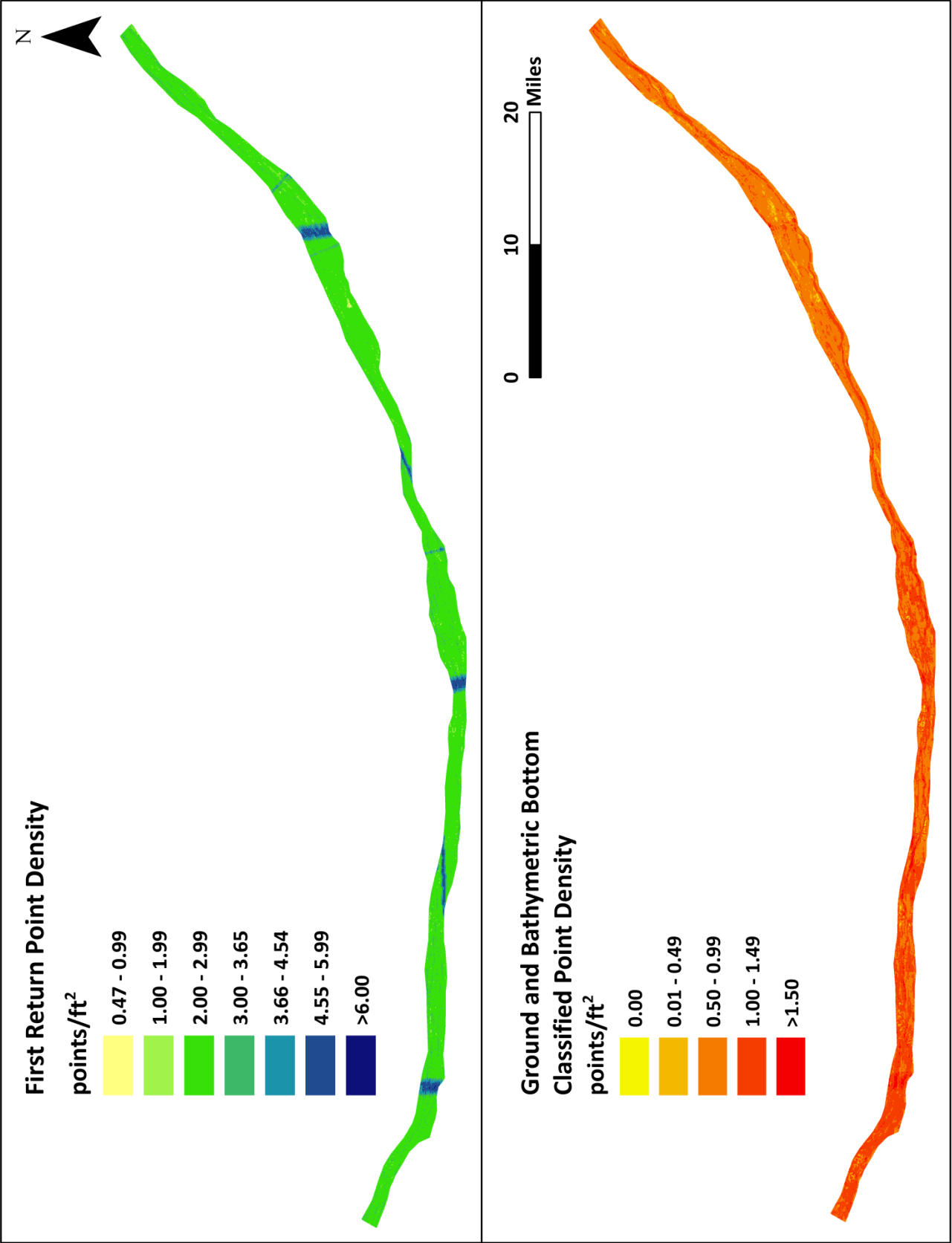


Figure 11: First return and ground and bathymetric bottom density map for the Platte River site (100 m x 100 m cells)

LiDAR Accuracy Assessments

The accuracy of the LiDAR data collection can be described in terms of absolute accuracy (the consistency of the data with external data sources) and relative accuracy (the consistency of the dataset with itself). See Appendix A for further information on sources of error and operational measures used to improve relative accuracy.

LiDAR Non-Vegetated Vertical Accuracy

Absolute accuracy was assessed using Non-vegetated Vertical Accuracy (NVA) reporting designed to meet guidelines presented in the FGDC National Standard for Spatial Data Accuracy³. NVA compares known ground quality assurance point data collected on open, bare earth surfaces with level slope (<20°) to the triangulated surface generated by the LiDAR points. NVA is a measure of the accuracy of LiDAR point data in open areas where the LiDAR system has a high probability of measuring the ground surface and is evaluated at the 95% confidence interval ($1.96 * RMSE$), as shown in Table 10.

The mean and standard deviation (sigma σ) of divergence of the ground surface model from ground check point coordinates are also considered during accuracy assessment. These statistics assume the error for x, y and z is normally distributed, and therefore the skew and kurtosis of distributions are also considered when evaluating error statistics. For the Platte River survey, 55 ground check points were withheld from the calibration and post-processing of the LiDAR point cloud, with resulting non-vegetated vertical accuracy of 0.183 feet (0.056 meters), with 95% confidence (Table 10, Figure 12). Additionally, bathymetric (submerged or along the water's edge), check points were also collected in order to assess the submerged surface vertical accuracy. Assessment of 288 bathymetric check points resulted in an average vertical accuracy of 0.382 feet (0.116 meters) at the 95th Percentile (Table 11, Figure 13).

QSI also assessed absolute accuracy using 1,018 ground control points. Although these points were used in the calibration and post-processing of the LiDAR point cloud, they still provide a good indication of the overall accuracy of the LiDAR dataset, and therefore have been provided in Table 10 and Figure 14.

³ Federal Geographic Data Committee, ASPRS POSITIONAL ACCURACY STANDARDS FOR DIGITAL GEOSPATIAL DATA EDITION 1, Version 1.0, NOVEMBER 2014. <http://www.asprs.org/PAD-Division/ASPRS-POSITIONAL-ACCURACY-STANDARDS-FOR-DIGITAL-GEOSPATIAL-DATA.html>.

Table 10: Absolute accuracy results

Non-Vegetated Vertical Accuracy		
	Ground Check Points	Ground Control Points
Sample	55 points	1,018 points
NVA (1.96*RMSE)	0.183 ft 0.056 m	0.192 ft 0.059 m
Average	0.011 ft 0.003 m	0.012 ft 0.004 m
Median	0.010 ft 0.003 m	0.020 ft 0.006 m
RMSE	0.093 ft 0.028 m	0.098 ft 0.030 m
Standard Deviation (1σ)	0.094 ft 0.029 m	0.097 ft 0.030 m

Table 11: Topobathymetric accuracy results

Topobathymetric Vertical Accuracy	
	Bathymetric Check Points
Sample	288 points
95 th Percentile	0.382 ft 0.116 m
Average	0.013 ft 0.004 m
Median	0.030 ft 0.009 m
RMSE	0.184 ft 0.056 m
Standard Deviation (1σ)	0.183 ft 0.056 m

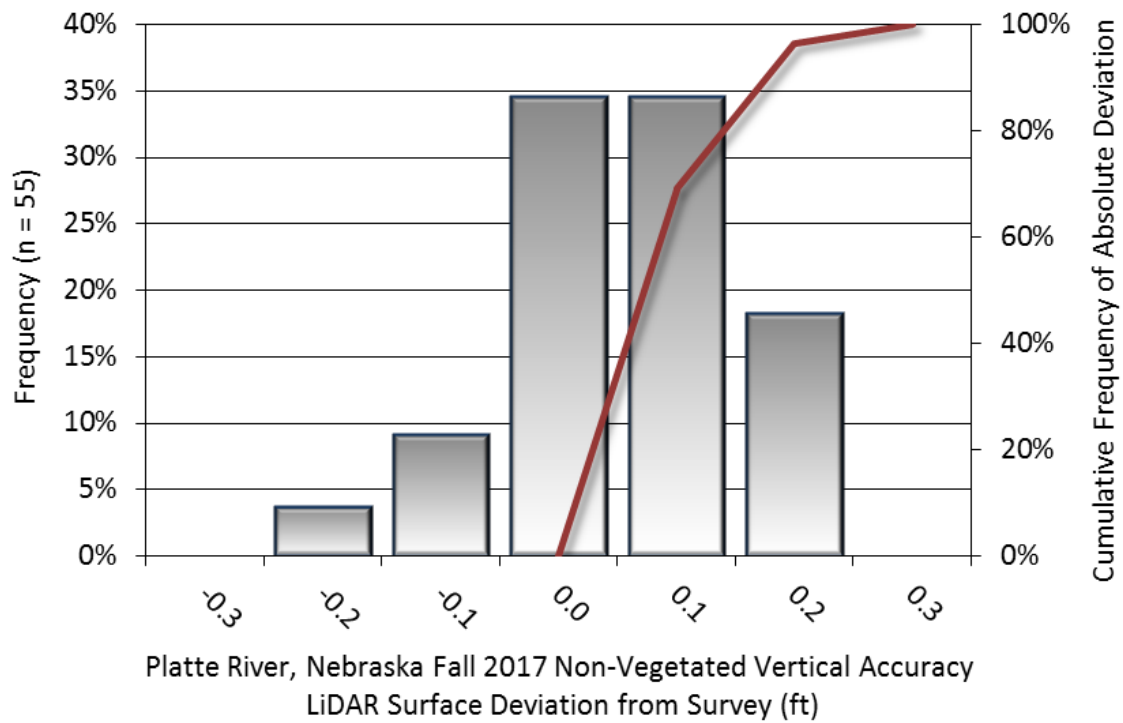


Figure 12: Frequency histogram for LiDAR surface deviation from ground check point values

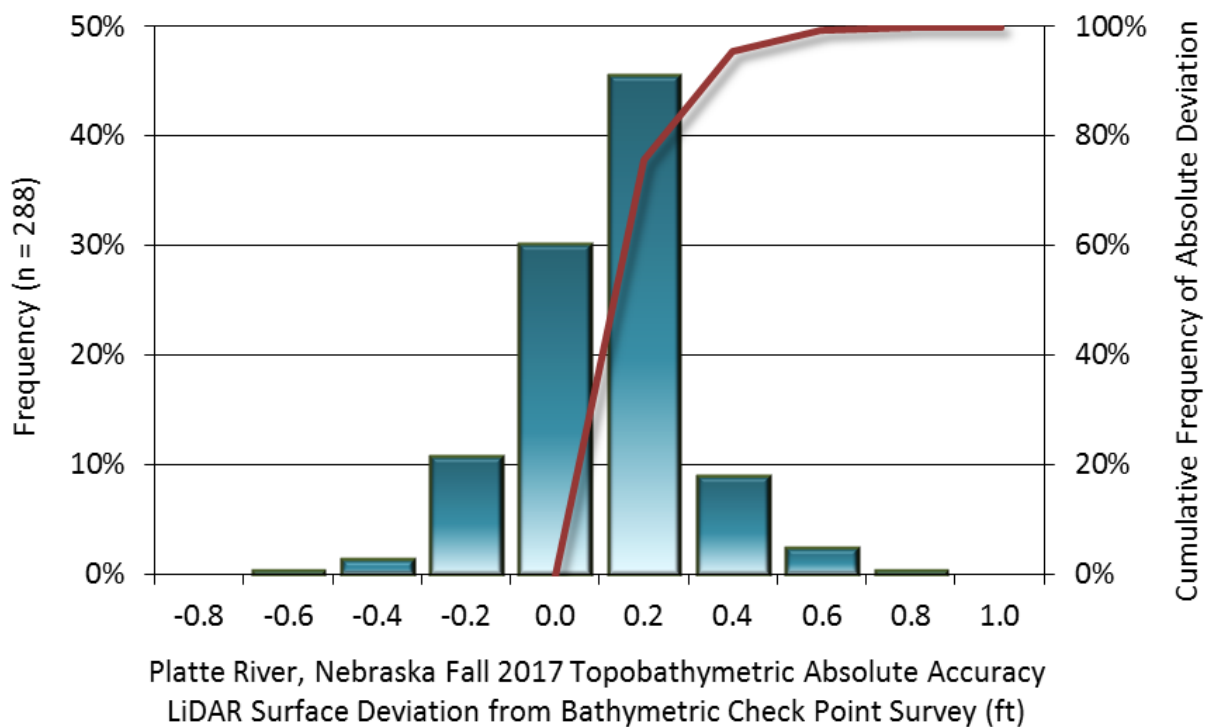


Figure 13: Frequency histogram for LiDAR surface deviation from bathymetric check point values

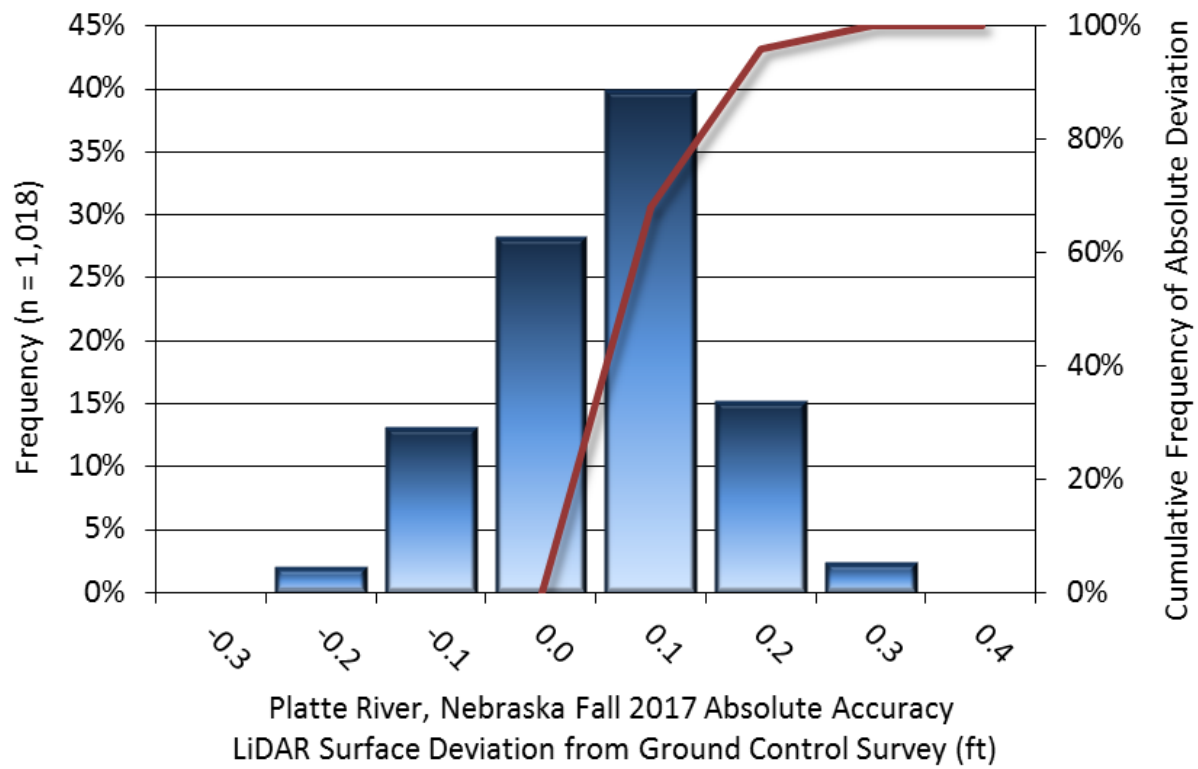


Figure 14: Frequency histogram for LiDAR surface deviation ground control point values

LiDAR Relative Vertical Accuracy

Relative vertical accuracy refers to the internal consistency of the data set as a whole: the ability to place an object in the same location given multiple flight lines, GPS conditions, and aircraft attitudes. When the LiDAR system is well calibrated, the swath-to-swath vertical divergence is low (<0.10 meters). The relative vertical accuracy was computed by comparing the ground surface model of each individual flight line with its neighbors in overlapping regions. The average (mean) line to line relative vertical accuracy for the Platte River LiDAR project was 0.059 feet (0.018 meters) (Table 12, Figure 15).

Table 12: Relative accuracy results

Relative Accuracy	
Sample	331 surfaces
Average	0.059 ft 0.018 m
Median	0.057 ft 0.018 m
RMSE	0.061 ft 0.019 m
Standard Deviation (1 σ)	0.013 ft 0.004 m
1.96 σ	0.025 ft 0.008 m

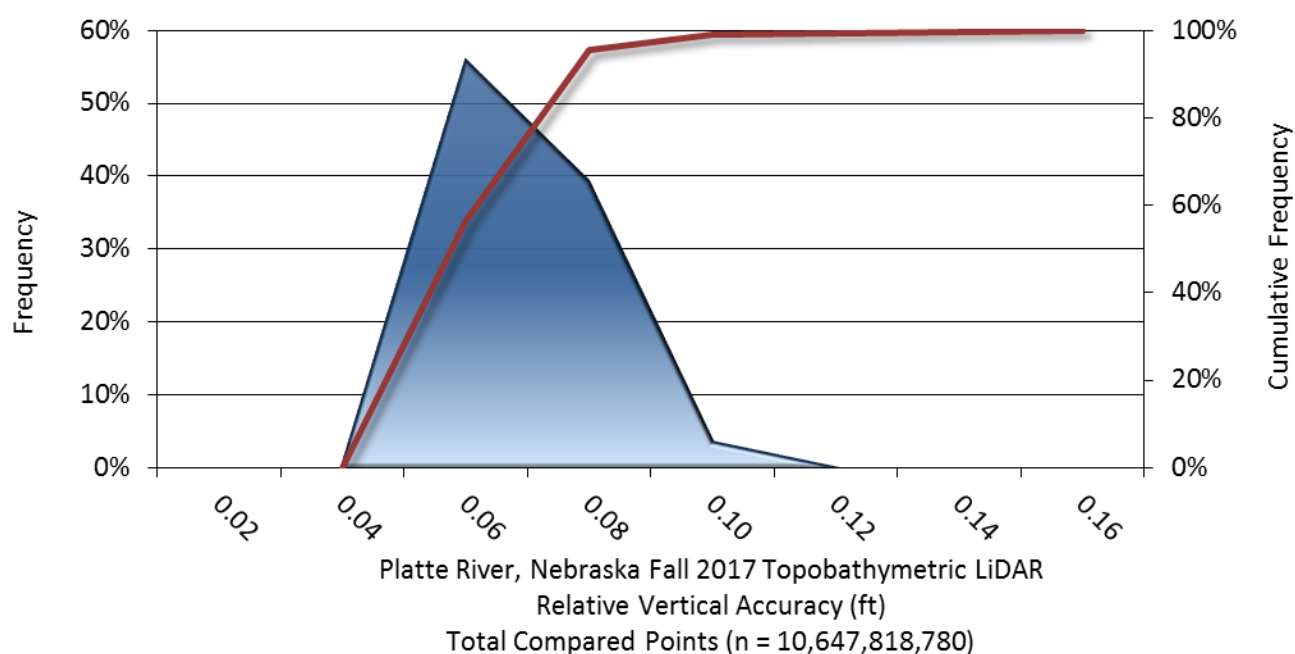


Figure 15: Frequency plot for relative vertical accuracy between flight lines

SELECTED IMAGES

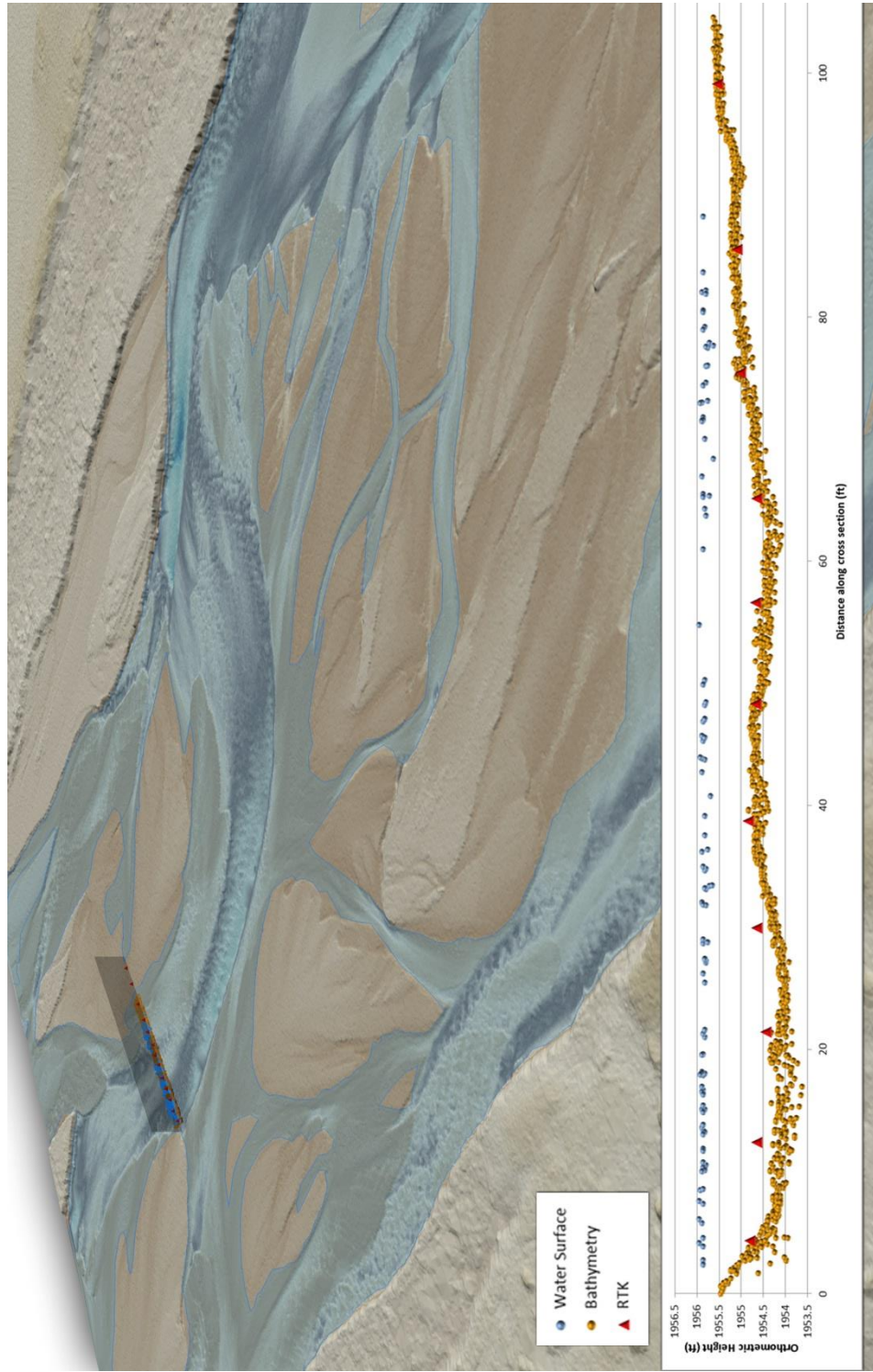


Figure 16: This image shows a view of the Platte River bathymetric bottom returns, with comparison chart showing congruency between bathymetric bottom returns, and collected bathymetric check point data. The image was created from the gridded topobathymetric bare earth model colored by elevation.

1-sigma (σ) Absolute Deviation: Value for which the data are within one standard deviation (approximately 68th percentile) of a normally distributed data set.

1.96 * RMSE Absolute Deviation: Value for which the data are within two standard deviations (approximately 95th percentile) of a normally distributed data set, based on the FGDC standards for Non-vegetated Vertical Accuracy (FVA) reporting.

Accuracy: The statistical comparison between known (surveyed) points and laser points. Typically measured as the standard deviation (sigma σ) and root mean square error (RMSE).

Absolute Accuracy: The vertical accuracy of LiDAR data is described as the mean and standard deviation (sigma σ) of divergence of LiDAR point coordinates from ground survey point coordinates. To provide a sense of the model predictive power of the dataset, the root mean square error (RMSE) for vertical accuracy is also provided. These statistics assume the error distributions for x, y and z are normally distributed, and thus we also consider the skew and kurtosis of distributions when evaluating error statistics.

Relative Accuracy: Relative accuracy refers to the internal consistency of the data set; i.e., the ability to place a laser point in the same location over multiple flight lines, GPS conditions and aircraft attitudes. Affected by system attitude offsets, scale and GPS/IMU drift, internal consistency is measured as the divergence between points from different flight lines within an overlapping area. Divergence is most apparent when flight lines are opposing. When the LiDAR system is well calibrated, the line-to-line divergence is low (<10 cm).

Root Mean Square Error (RMSE): A statistic used to approximate the difference between real-world points and the LiDAR points. It is calculated by squaring all the values, then taking the average of the squares and taking the square root of the average.

Data Density: A common measure of LiDAR resolution, measured as points per square meter.

Digital Elevation Model (DEM): File or database made from surveyed points, containing elevation points over a contiguous area. Digital terrain models (DTM) and digital surface models (DSM) are types of DEMs. DTMs consist solely of the bare earth surface (ground points), while DSMs include information about all surfaces, including vegetation and man-made structures.

Intensity Values: The peak power ratio of the laser return to the emitted laser, calculated as a function of surface reflectivity.

Nadir: A single point or locus of points on the surface of the earth directly below a sensor as it progresses along its flight line.

Overlap: The area shared between flight lines, typically measured in percent. 100% overlap is essential to ensure complete coverage and reduce laser shadows.

Pulse Rate (PR): The rate at which laser pulses are emitted from the sensor; typically measured in thousands of pulses per second (kHz).

Pulse Returns: For every laser pulse emitted, the number of wave forms (i.e., echoes) reflected back to the sensor. Portions of the wave form that return first are the highest element in multi-tiered surfaces such as vegetation. Portions of the wave form that return last are the lowest element in multi-tiered surfaces.

Real-Time Kinematic (RTK) Survey: A type of surveying conducted with a GPS base station deployed over a known monument with a radio connection to a GPS rover. Both the base station and rover receive differential GPS data and the baseline correction is solved between the two. This type of ground survey is accurate to 1.5 cm or less.

Post-Processed Kinematic (PPK) Survey: GPS surveying is conducted with a GPS rover collecting concurrently with a GPS base station set up over a known monument. Differential corrections and precisions for the GNSS baselines are computed and applied after the fact during processing. This type of ground survey is accurate to 1.5 cm or less.

Scan Angle: The angle from nadir to the edge of the scan, measured in degrees. Laser point accuracy typically decreases as scan angles increase.

Native LiDAR Density: The number of pulses emitted by the LiDAR system, commonly expressed as pulses per square meter.

APPENDIX A - ACCURACY CONTROLS

Relative Accuracy Calibration Methodology:

Manual System Calibration: Calibration procedures for each mission require solving geometric relationships that relate measured swath-to-swath deviations to misalignments of system attitude parameters. Corrected scale, pitch, roll and heading offsets were calculated and applied to resolve misalignments. The raw divergence between lines was computed after the manual calibration was completed and reported for each survey area.

Automated Attitude Calibration: All data were tested and calibrated using TerraMatch automated sampling routines. Ground points were classified for each individual flight line and used for line-to-line testing. System misalignment offsets (pitch, roll and heading) and scale were solved for each individual mission and applied to respective mission datasets. The data from each mission were then blended when imported together to form the entire area of interest.

Automated Z Calibration: Ground points per line were used to calculate the vertical divergence between lines caused by vertical GPS drift. Automated Z calibration was the final step employed for relative accuracy calibration.

LiDAR accuracy error sources and solutions:

Type of Error	Source	Post Processing Solution
GPS (Static/Kinematic)	Long Base Lines	None
	Poor Satellite Constellation	None
	Poor Antenna Visibility	Reduce Visibility Mask
Relative Accuracy	Poor System Calibration	Recalibrate IMU and sensor offsets/settings
	Inaccurate System	None
Laser Noise	Poor Laser Timing	None
	Poor Laser Reception	None
	Poor Laser Power	None
	Irregular Laser Shape	None

Operational measures taken to improve relative accuracy:

Low Flight Altitude: Terrain following was employed to maintain a constant above ground level (AGL). Laser horizontal errors are a function of flight altitude above ground (about 1/3000th AGL flight altitude).

Focus Laser Power at narrow beam footprint: A laser return must be received by the system above a power threshold to accurately record a measurement. The strength of the laser return (i.e., intensity) is a function of laser emission power, laser footprint, flight altitude and the reflectivity of the target. While surface reflectivity cannot be controlled, laser power can be increased and low flight altitudes can be maintained.

Reduced Scan Angle: Edge-of-scan data can become inaccurate. The scan angle was reduced to a maximum of $\pm 20^\circ$ from nadir, creating a narrow swath width and greatly reducing laser shadows from trees and buildings.

Quality GPS: Flights took place during optimal GPS conditions (e.g., 6 or more satellites and PDOP [Position Dilution of Precision] less than 3.0). Before each flight, the PDOP was determined for the survey day. During all flight times, a dual frequency DGPS base station recording at 1 second epochs was utilized and a maximum baseline length between the aircraft and the control points was less than 13 nm at all times.

Ground Survey: Ground survey point accuracy (<1.5 cm RMSE) occurs during optimal PDOP ranges and targets a minimal baseline distance of 4 miles between GPS rover and base. Robust statistics are, in part, a function of sample size (n) and distribution. Ground survey points are distributed to the extent possible throughout multiple flight lines and across the survey area.

50% Side-Lap (100% Overlap): Overlapping areas are optimized for relative accuracy testing. Laser shadowing is minimized to help increase target acquisition from multiple scan angles. Ideally, with a 50% side-lap, the nadir portion of one flight line coincides with the swath edge portion of overlapping flight lines. A minimum of 50% side-lap with terrain-followed acquisition prevents data gaps.

Opposing Flight Lines: All overlapping flight lines have opposing directions. Pitch, roll and heading errors are amplified by a factor of two relative to the adjacent flight line(s), making misalignments easier to detect and resolve.